Optimisation of active SHM system based on optimal number and placement of piezoelectric transducers

Ali H Daraji
School of Mechanical, Aerospace and Automotive Engineering, Coventry University, UK
Email: ac7202@coventry.ac.uk

Jianqiao Ye
Engineering Department, Lancaster University, Lancaster, UK
Email: j.ye2@lancster.ac.uk

Jack M Hale
School of Engineering, Newcastle University, UK
Email: jack.hale@ncl.ac.uk

ABSTRACT

This paper concerns optimal placement and number of discrete piezoelectric macro fibre composite (MFC) sensors to optimise SHM systems. Its novelty lies in a two-stage placement methodology for discrete piezoelectric transducers, with fitness and objective functions to optimise the location and number of discrete piezoelectric sensors in order to reduce the cost and complexity of data processing and increase the effectiveness in damage detection. The maximisation of sensor voltage amplitude at multiple modes of vibration and the average of sensor normal damage index $RMSD^{nor}$ measured for several plates artificially cracked at different positions and orientations are proposed as objective functions to optimise the locations and the number of efficient piezoelectric sensors. A non-normalised root-mean-square deviation $RMSD$ is introduced in this study in place of the conventional normalised $NRMSD$ to assess the degree of damage and sensor effectiveness. Furthermore, normal damage indices $RMSD^{nor}$ and $NRMSD^{nor}$ normalised to 100% are proposed as the fitness functions. The placement methodology is utilised and verified for stiffened and unstiffened plates; stiffeners are used to break the dynamic symmetry and increase plate complexity. The performance of the placement methodology is tested for a healthy and twelve damaged plates to optimise SHM system based on the maximisation of sensor voltage and average normal damage index $RMSD^{nor}$ as objective functions. The results show that the placement methodology is efficient in determining the optimum number and placement of piezoelectric sensors at a low computational effort. The optimum placement of two piezoelectric sensors can efficiently monitor the crack's initiation at different positions and multiple modes of vibration. The optimal placement and number of sensors have a positive impact on the cost, data acquisition and processing of the active SHM system

Keywords, piezoelectric, optimal placement, genetic algorithms, normal damage index, SHM

1. INTRODUCTION

High specific strength structures are progressively employed in the engineering industry to optimise loading capacity, structural weight, material cost and fuel consumption. These structures are subjected to dynamic loading, which can cause failure due to internal or external micro-cracks. It requires continuous observation and online monitoring for early detection of microcracks before failure occurs to save cost, maintenance and lives. The motivation of this study is attributable to the lack of investigation on the optimal placement and number of piezoelectric transducers for active structural health monitoring systems under low frequencies. Another motivating research topic is to find an alternative damage index to assess the degree of damage instead of the Root Mean Square Deviation normalised to dimensionless values (NRMSD). Optimising the number and placement of piezoelectric sensors for an active structural health monitoring (SHM) system is a challenging research topic that needs to be considered in the earliest structure design stage to reduce the cost and complexity of data processing and increase their effectiveness in damage detection.

Nondestructive test methods for local damage detection have been conducted by either visual or localised experimental techniques such as acoustic or ultrasonic, magnetic field, radiographs, eddy-current or thermal field methods. Apart from ultrasonics, these methods detect local damage on or near the surface of the structure, but not delamination or internal cracks (Doebling *et al.*, 1996). Conventional ultrasonic and acoustic methods are labour intensive, time-consuming and not efficient for a large area (Soni, Das and Chattopadhyay, 2009). Structural Health Monitoring (SHM) is a more efficient and global damage detecting scheme for identifying hidden and incipient micro-cracks for simple and complex structures based on monitoring of dynamic characteristics using a set of sensors and data acquisition system (Doebling *et al.*, 1996; Soni, Das and Chattopadhyay, 2009; Soni, Das and Chattopadhyay, 2009) , and may incorporate real-time diagnosis of potential damage during the early stages of crack formation (Chalioris *et al.*, 2015).

Cracks cause a change in structural stiffness, damping, natural frequencies and modal responses that might be observed, providing sensors of an appropriate type are used at appropriate locations. Piezoelectric transducers have been used for SHM of large structures due to their virtues of active sensing, quick response, low cost and availability in different shapes (Song *et al.*, 2007). Their effectiveness for microcrack detection could be enhanced by optimising their locations.

Khatir et al presented an inverse algorithm based on proper orthogonal decomposition and radial basis function to evaluate single and multiple cracks identification in plate structure bonded strain sensors (Khatir and Abdel Wahab, 2019). Also, they proposed a two stages approach for damage assessment based on modal strain energy indicator coupled with teaching-learning optimisation algorithm and isogeometric analysis (Khatir *et al.*, 2019). The method of cracks identification was then improved by training the artificial neural network parameters using the Jaya algorithm, extended isogeometric analysis to improve the accuracy based on frequency and strain measurements (Khatir *et*

al., 2020). Gillich et al proposed a damage assessment method based on multi-modal analysis to evaluate the damage in beams subjected to an axial force induced by temperature changes (Gillich *et al.*, 2019).

Optimisation of placement and number of piezoelectric sensors in active SHM systems is a significant research topic. It aims to reduce the complexity and cost of data acquisition and health monitoring systems and increase their effectiveness in damage detection. The most recent reviewing article by Ostachowicz and Soman had reported that the optimisation of sensor placement reduces the cost and enhances the quality of the SHM system. They had stated that optimisation of sensor placement is still challenging at present and needs well-coordinated interdisciplinary research, and should be tackled at the earliest stages of structure design (Ostachowicz and Soman, 2019). Flynn and Todd utilised the optimal placement of sensor and actuator in active SHM strategies to optimise the performance of the damage detector using ultrasonic waves (Flynn and Todd, 2010b). The main elements affecting the performance of the SHM system are sensors, data acquisition and degree of damage evaluation. It has been shown that optimal sensor location plays a crucial role in the maximisation of the performance and cost reduction of the SHM system using accelerometer sensors (Markmiller and Chang, 2010; Li, Li and Fritzen, 2012; Lu *et al.*, 2016). The accurate identification of structure behaviour in SHM is directly affected by the number and position of sensors (Soni, Das and Chattopadhyay, 2009; Flynn and Todd, 2010b; Yang *et al.*, 2012), and optimal placement has a significant effect on the performance of the SHM system (Li, Li and Fritzen, 2012; Yi, Li and Gu, 2011; Buff *et al.*, 2012). He et al have identified sensor placement as an essential aspect of SHM of a bridge structure but found some defects in existing methods using a single optimal index, with a selection of modal order and sensor number chosen on the basis of experience and requiring long computational time (He *et al.*, 2013). They proposed a hybrid optimisation based adaptive genetic algorithm to address these limitations. Genetic algorithms based on the minimisation of Bayes risk as an objective function were employed by Flynn and Todd to optimise the location of piezoelectric sensors and actuators for ultrasonics in a plate (Flynn and Todd, 2010a). The optimal placement of accelerometer sensors have been thoroughly investigated for SHM of small and large scale structures using genetic algorithms based on the maximisation of the probability of crack detection(Markmiller and Chang, 2010), off-diagonal element of modal assurance criterion matrix (He *et al.*, 2013; Zhou *et al.*, 2015; Zhu *et al.*, 2016) and mean square deviation of natural frequencies as fitness functions (Mehrjoo, Khaji and Ghafory-Ashtiany, 2013; Mehrjoo, Khaji and Ghafory-Ashtiany, 2013). Similarly, the optimal placement of piezoelectric sensors and actuators using genetic algorithms bonded on beams (Zhang *et al.*, 2000; Kumar and Narayanan, 2008), plates (Sadri, Wright and Wynne, 1999; Han and Lee, 1999; Ramesh Kumar and Narayanan, 2007; Daraji and Hale, 2012; Daraji and Hale, 2014) and proposed placement method using Ansys package (Daraji, Hale and Ye, 2018) are thoroughly investigated for active vibration control, but there is a lack of study for active structure health monitoring.

Concrete, fibre reinforced composite, and steel structures work under dynamic loading and suffer from mass variation due to environmental erosion. Piezoelectric electromechanical impedance (EMI) technology and $NMRSD$ have been used to inspect, monitor and evaluate the damage of these structures at ultrasonic frequencies (Park *et al.*, 2006; Lee and Park, 2012; Yang, 2010; Song, Lim and Sohn, 2013; Kong *et al.*, 2016). It has been noticed in the published work that the results of $NRMSD$ show little diversity and tend to cluster close to being identical values for different sensor locations, cracks and ranges of frequencies. Guo et al have experimentally investigated the health monitoring of concrete structures with embedded piezoelectric sensors based on the spectrum of EMI frequency response and $NRMSD$. The authors evaluated the effects of adding masses at different locations using ultrasonic frequencies and found that the results of the $NRMSD$ damage indices are identical (Guo *et al.*, 2016). Similarly, concrete health monitoring with eight embedded piezoelectric sensors was tested experimentally under gradually increased loading, producing two damages. The sensors recorded nearly identical $NRMSD$ indices for both damages (Chalioris *et al.*, 2015). Fan et al investigated damage evaluation of a concrete beam and found similar $NRMSD$ indices for a piezoelectric sensor located at different positions on a cracked concrete beam. They reported that $NRMSD$ is widely used to evaluate structural damage but does not provide quantitative information about the structure damages and proposed a volumetric crack index for better performance (Fan *et al.*, 2018). Perera et al have proposed a methodology for damage identification based on a combination of linear mixed methods with EMI using root mean square deviation normalised to dimensionless value with application to a concrete beam bonded with piezoelectric sensors (Perera *et al.*, 2021). Balamonica et al have proposed a multi-sensing technique for crack and damage detection for a concrete structure bonded with piezoelectric sensors connected in series and parallel (Balamonica *et al.*, 2020). A moving root mean square deviation normalised to dimensionless, moving mean absolute error and cross-correlation were used as dynamic metrics for damage evaluation. Ai et al investigated cracks and damage detection in a concrete structure using an embedded rather than surface mounted piezoelectric sensor to filter the external impact and the environmental effects. A slope-based RMSD normalised to dimensionless was used to evaluate both types of piezoelectric sensors (Ai, Zhu and Luo, 2016).

In this study, an alternative non-normalised root mean square deviation is proposed to eliminate these drawback effects of the $NRMSD$ damage index. This is represented by the average of square root error of the sensors bonded on a healthy and unhealthy structure ($RMSD$) and normal $RMSD^{nor}$ normalised to 100% damage indices. Based on the authors' best knowledge, most published work in SHM systems either use genetic algorithms to optimise the location of accelerometer sensors or piezoelectric transducers randomly located. There is a lack of research on the optimal placement and number of piezoelectric transducers to optimise the structural health monitoring systems.

This study proposes a fitness function, objective function, and two stages placement methodology to optimise the location and number of piezoelectric transducers using genetic algorithms. The first stage of the placement methodology was applied for a cantilever composite plate and plate stiffened by beam to optimise the locations of discrete MFC sensors covering 4.5% of the plate's surface area using the maximisation of the sensor amplitude voltage as an objective function. The second stage was applied to healthy and twelve damaged plates to find the optimal placement and number of sensors using the maximisation of the average normal damage index $RMSD^{nor}$ as an objective function.

2. MODELLING

High specific strength structures are mostly constructed as thin shells or plates stiffened by beams to optimise loading capacity, fuel consumption and material cost. The dynamic equilibrium equations in the uncoupled state-space form for a flat plate and plate stiffened by beams bonded with piezoelectric transducers are given by (Daraji and Hale, 2014):

$$\dot{\boldsymbol{X}} = \boldsymbol{A}\boldsymbol{X} + \boldsymbol{B}_1\boldsymbol{V}_a + \boldsymbol{B}_2\boldsymbol{F} + \boldsymbol{B}_3\boldsymbol{r} \tag{1}$$

$$\boldsymbol{V}_s = \boldsymbol{C}\,\boldsymbol{X} \tag{2}$$

Where $\boldsymbol{A}, \boldsymbol{C}, \boldsymbol{B}_1, \boldsymbol{B}_2$ and $\boldsymbol{B}_3$ are modal state, piezoelectric sensor, actuator, external mechanical force excitation and base motion excitation matrices, respectively. $\boldsymbol{X}, \boldsymbol{V}_s, \boldsymbol{V}_a, \boldsymbol{F}$ and $\boldsymbol{r}$ denote modal state, sensor voltage, actuator voltage excitation, external mechanical force excitation and external motion base excitation vectors, respectively. For a single mode of vibration ω_i, these matrices are defined according to the following equations:

$$\boldsymbol{X} = \{\omega_i\eta_i \quad \dot{\eta}_i\}^{\mathrm{T}} \quad , \quad \dot{\boldsymbol{X}} = \{\omega_i\dot{\eta}_i \quad \ddot{\eta}_i\}^{\mathrm{T}} \tag{3}$$

$$\boldsymbol{A}_i = \begin{bmatrix} 0 & \omega_i \\ -\omega_i & -2\xi_i\omega_i \end{bmatrix} \tag{4}$$

$$\boldsymbol{B}_{1i} = \begin{bmatrix} \boldsymbol{0} \\ -\boldsymbol{\varphi}^{\boldsymbol{T}}\boldsymbol{K}_{u\emptyset} \end{bmatrix} \quad , \quad \boldsymbol{B}_{2i} = \begin{bmatrix} 0 \\ \boldsymbol{\varphi}^{\mathrm{T}} \end{bmatrix} \quad , \quad \boldsymbol{B}_{3i} = \begin{bmatrix} 0 \\ -\boldsymbol{\varphi}^{\mathrm{T}}\boldsymbol{\omega}^{\boldsymbol{2}}\boldsymbol{I} \end{bmatrix} \tag{5}$$

$$\boldsymbol{C}_i = \begin{bmatrix} -\boldsymbol{\varphi}^{\mathbf{T}}\boldsymbol{\omega}_{\boldsymbol{i}}^{-\mathbf{1}}\, C_s^{-1}\boldsymbol{K}_{u\emptyset} & 0 \end{bmatrix} \tag{6}$$

Where the subscripts $i, s, a,$ and I and ξ represent the mode number, sensor and actuator, identity matrix and structural damping ratio, respectively. The mass normalised modal matrix $\boldsymbol{\varphi}$ is obtained by solving the free vibration of undamped structure for each frequency ω, and η is a single vector of the modal coordinate. The piezoelectric electromechanical coupling is denoted by $\boldsymbol{K}_{u\emptyset}$ and piezoelectric capacitance by C_s. The state, sensor and actuator matrices for n_m modes and r_a sensors and actuators are given by:

$$\boldsymbol{A}_{(2n_m \times 2n_m)} = \begin{bmatrix} \boldsymbol{A}_1 & \cdots & 0 \\ \vdots & \ddots & \vdots \\ 0 & \cdots & \boldsymbol{A}_{n_m} \end{bmatrix} \tag{7}$$

$$\boldsymbol{B}_{1(2n_m \times r_a)} = \begin{bmatrix} (\boldsymbol{B}_1)_1 & \cdots & (\boldsymbol{B}_1)_{r_a} \\ \vdots & \cdots & \vdots \\ (\boldsymbol{B}_1)_{nm} & \cdots & (\boldsymbol{B}_1)_{r_a} \end{bmatrix} \tag{8}$$

$$\boldsymbol{C}_{(r_a \times 2n_m)} = \begin{bmatrix} (\boldsymbol{C})_1 & \cdots & (\boldsymbol{C})_{nm} \\ \vdots & \cdots & \vdots \\ (\boldsymbol{C})_{r_a} & \cdots & (\boldsymbol{C})_{r_a} \end{bmatrix} \tag{9}$$

$$\boldsymbol{X}_{(2n_m \times 1)} = \{\omega_1 \eta_1 \quad \dot{\eta}_1 \quad \cdots \quad \omega_{n_m} \eta_{n_m} \quad \dot{\eta}_{n_m}\}^T \tag{10}$$

3. DAMAGE EVALUATION INDICES

In this study, the non-normalised root-mean-square deviation RMSD index is proposed to evaluate the degree of damage of a structure based on the difference between the signature of the sensor voltage frequency response for the healthy structure and the response of the damaged plate. Figure (1) shows sensor voltage frequency responses for both healthy and unhealthy structures to clarify the formulas for the damage assessment $RMSD$ and $NRMSD$ indices. Equations (11) and (12) represent both damage evaluation indices, where $V_{hj}, V_{cj}, i, j \; and \; n$ denote the sensor voltages for healthy and cracked plates, optimal sensor position, measuring sensor voltage point at a specific frequency, and the total number of measurement points, respectively.

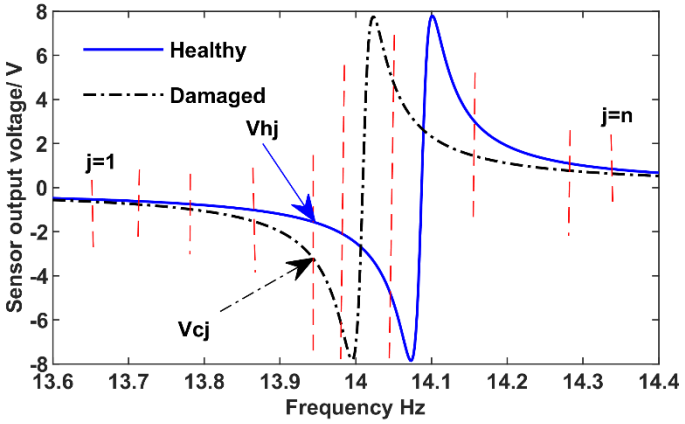

Fig. 1. Piezoelectric sensor voltage frequency response for healthy and damage structures

Equation (11) of $NRMSD$ shows the numerator is divided by the piezoelectric sensor voltage squared value, resulting in a larger damage index value for a sensor located at an ineffective position than a sensor located at an efficient higher dynamic strain position. The $NRMSD$ damage index might conflict with the piezoelectric sensor optimisation schemes, mislead crack evaluation, and cluster the

results to the same degree of damage. The non-normalised $RMSD$ index is expected to be more reliable than $NRMSD$ for the damage evaluation of a structure under low frequencies.

$$NRMSD_i = \sqrt{\frac{\sum_{j=1}^{j=n}(V_{hj} - V_{cj})^2}{\sum_{j=1}^{j=n} {V_{hj}}^2}} \tag{11}$$

$$RMSD_i = \sqrt{\frac{\sum_{j=1}^{j=n}(V_{hj} - V_{cj})^2}{n}} \tag{12}$$

4. OBJECTIVE FUNCTION

This study proposes fitness and objective functions for the determination of the optimal placement and number of piezoelectric transducers based on the maximisation of sensor output voltage and the average normal damage index for healthy and damaged structures subjected to external excitation. Consider the state space equation (1), which describes the dynamic motion of a structure under external actuator voltage $\boldsymbol{V}_a$, mechanical force $\boldsymbol{F}$ and base motion $\boldsymbol{r}$ excitations:

$$\dot{\boldsymbol{X}} = \boldsymbol{AX} + \boldsymbol{B}_1\boldsymbol{V}_a + \boldsymbol{B}_2\boldsymbol{F} + \boldsymbol{B}_3\boldsymbol{r} \tag{13}$$

Firstly, the optimal sensor placement is investigated for a structure under base motion excitation $\boldsymbol{r}$ to find the optimal sensor location. Taking the Laplace transforms of both sides of equation (13), after eliminating the effects of the external actuator excitation voltage $\boldsymbol{V}_a$ and the external excitation force$\boldsymbol{F}$, yields:

$$\boldsymbol{sX}(s) = \boldsymbol{AX}(s) + \boldsymbol{B}_3\boldsymbol{r}(s) \tag{14}$$

$$\boldsymbol{X}(s) = \boldsymbol{B}_3\boldsymbol{r}(s)\ (\boldsymbol{s} - \boldsymbol{A})^{-1} \tag{15}$$

Also, from equation (2), the sensor outputs are given by:

$$\boldsymbol{V}_s = \boldsymbol{CX} \tag{16}$$

Taking the Laplace transform of equation (16) results in:

$$\boldsymbol{V}_s(s) = \boldsymbol{CX}(s) \tag{17}$$

From equations (17) and (15):

$$\boldsymbol{V}_s(s) = \boldsymbol{C}\ (\boldsymbol{s} - \boldsymbol{A})^{-1}\ \boldsymbol{B}_3\boldsymbol{r}(s) \tag{18}$$

The output sensor voltage in the frequency domain at a single mode of vibration is:

$$\boldsymbol{V}_s = \boldsymbol{C}(j\boldsymbol{\omega}\boldsymbol{I} - \boldsymbol{A})^{-1}\boldsymbol{B}_3\boldsymbol{r} \tag{19}$$

The output voltage of the sensor n_s as a result of applying external base motion excitation $\boldsymbol{r}$ at multiple modes of vibration n_m is:

$$\boldsymbol{V}_s(n_s, n_m) = \boldsymbol{C}(j\boldsymbol{\omega I} - \boldsymbol{A})^{-1}\boldsymbol{B}_3\,\boldsymbol{r} \tag{20}$$

Secondly, the optimal sensor placement is considered for the structure under external force excitation or voltage excitation. In the same way, the sensor voltage is calculated as a result of applying external force $\boldsymbol{F}$ and voltage excitation $\boldsymbol{V}_a$ at multiple modes of vibration n_m are:

$$\boldsymbol{V}_s(n_s, n_m) = \boldsymbol{C}(j\boldsymbol{\omega I} - \boldsymbol{A})^{-1}\boldsymbol{B}_2\boldsymbol{F} \tag{21}$$

$$\boldsymbol{V}_s(n_s, n_m) = \boldsymbol{C}(j\boldsymbol{\omega I} - \boldsymbol{A})^{-1}\boldsymbol{B}_1\boldsymbol{V}_a \tag{22}$$

The total voltage $V_s(x, y)$ of the sensors under multiple modes of vibration are the fitness function, i.e.,

$$V_s(x, y) = \sum_{j=1}^{n_m}\sum_{i=1}^{n_s}\boldsymbol{V}_s(i, j) \tag{23}$$

$$J^P(x, y) = \max(V_s(x, y)) \tag{24}$$

Equation (24) represents an objective function under the condition of x and $y\,\epsilon$ structural dimensions to find the optimal sensor location as a first stage of placement optimisation. However, the second optimisation stage is based on the proposed normal damage index to select the best transducers. The $RMSD$ damage index is considered as a fitness function to measure the effectiveness of the optimal sensors in damage detection based on sensor voltage frequency responses for healthy and cracked structures at different positions and orientations according to the following formula.

$$RMSD_i = \sqrt{\frac{\sum_{j=1}^{j=n}(V_{hj} - V_{cj})^2}{n}} \tag{25}$$

The proposed normal $RMSD_i^{nor}$ damage index for each optimal sensor i is evaluated at different crack positions by dividing the sensor damage index $RMSD_i$ for the optimal sensors n_s by the maximum sensor damage index $RMSD_{max}$ normalised to 100%, according to the following equation:

$$RMSD_i^{nor} = \frac{RMSD_i}{RMSD_{max}} \tag{26}$$

The effective number of the optimum sensors is selected based on the average normal damage index ($RMSD_i^{nor}$) for several plates cracked at different positions and orientations (n_p), which is considered as an objective function $J^N(x, y)$ to be larger than 90% according to the equation (27). The

percentage is chosen 90% based on structural dimensions and design requirements to reduce the cost and simplify the complexity of data analysis in the active SHM system.

$$J^N(x,y) = \frac{\sum_{i=1}^{i=n_p} RMSD_i^{nor}(x,y)}{n_p} \geq 90\% \quad (27)$$

5. PLACEMENT METHODOLOGY

In this study, the plate discretised into one hundred thirty possible sites, and it is obvious that there are one hundred thirty places to locate a single sensor (130 combinations) and only one combination for placing one hundred thirty sensors (one in every location). The number of combinations rises exponentially to reach the maximum in optimising sixty-five sensors (half of the total positions on the plate), cause the optimisation problem to become more complex and requiring high computational effort in finding the suboptimal or optimal solution. For example, the location of six sensors has 5.9×10^9 candidate solutions, of which just one is the optimal. It is impractical to evaluate the effectiveness of every possible solution. Therefore, the genetic algorithm is considered as a powerful guided search method to find the optimal solution, though this is still challenging to find the global optimal solution for large possible combinations. Another complexity for the current case study is to extend the genetic algorithms placement methodology to cover several damaged plates marked by cracks at different positions and orientations. Therefore, this study proposes a two-stage placement methodology including fitness and objective functions to find the global optimal solution representing the optimal number and placement of sensors with the minimum computational effort.

Optimal location of sensors for an application such as this is both desirable and challenging. It is clearly desirable to limit the number of sensors to keep down the cost and the complexity of the data analysis, but this can only be done if they are placed effectively to detect and characterise damage at all locations on the structure.

Optimisation problems of this type are well suited to the genetic algorithm. This is a well-known technique based on biological natural selection, by which a population of potential solutions evolves over numerous generations to converge on an optimally "fit" solution. The genetic algorthim is fully described by (Goldberg D. E., 1989) but briefly the solution to a problem, in this case, the locations of n_s sensors, is coded as a string of integer numbers analogous to the genetic code on a DNA string or chromosome. A "breeding population" of a number of individuals is set up, each characterised by its chromosome. The "fitness" of each individual is determined according to some fitness function, in this case the output of the sensors over a range of vibration frequencies, after which the population "breeds" by pairing individuals and combining their chromosomes to generate "children" for the next generation. There are many different breeding strategies, but all ensure that high fitness individuals are favoured in the breeding process, as in nature, so that useful genes tend to propagate through the generations and

detrimental genes disappear. There is also a small amount of mutation of the chromosomes during breeding, which helps to ensure diversity in the population and prevent premature convergence. By this means, a large search space can be explored quite efficiently and a global optimum obtained relatively quickly. A genetic algorithm program was written using MatLab m-code and the finite element package ANSYS for this work, according to the following flowchart:

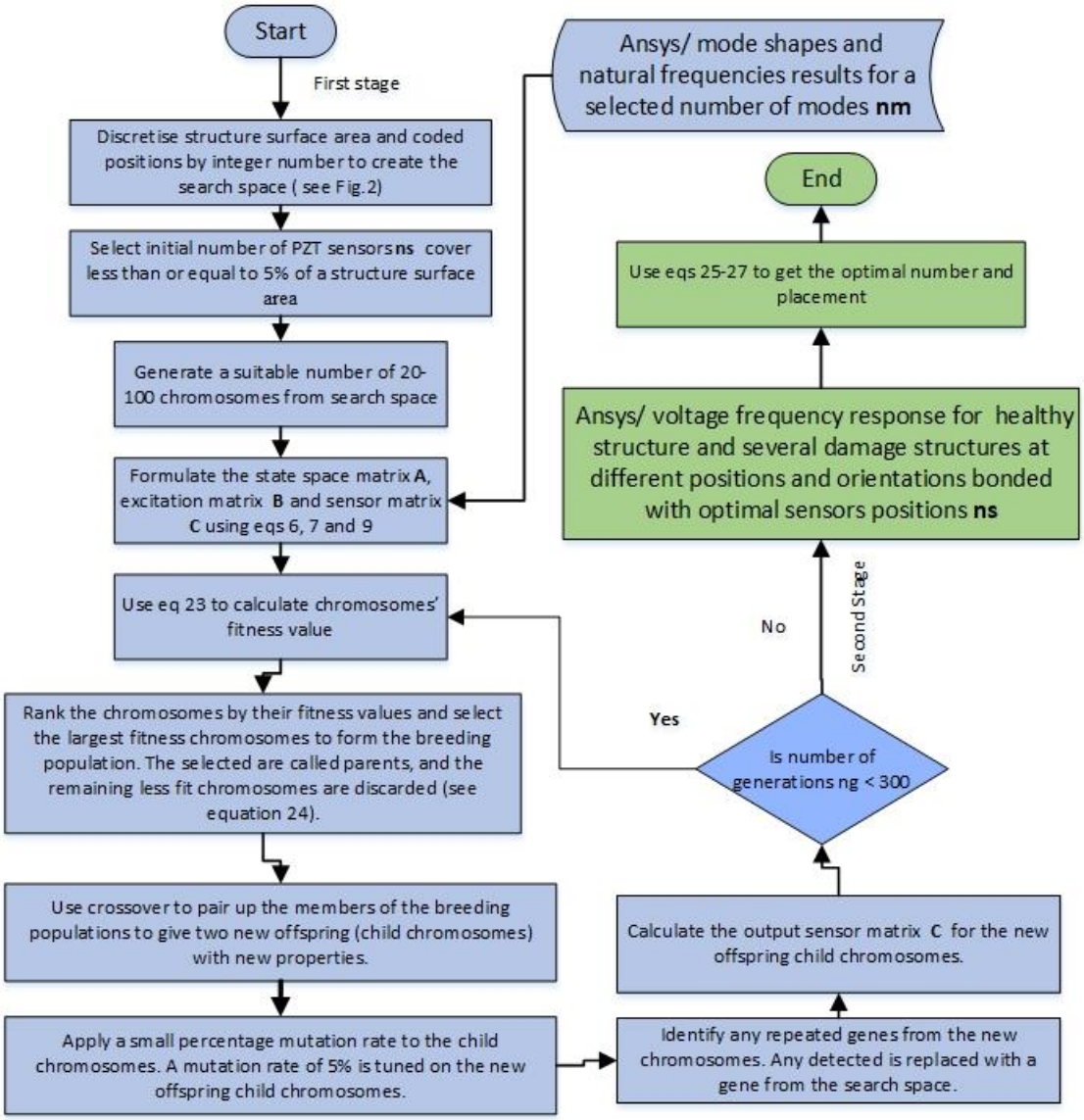

6. RESULTS AND DISCUSSION

In this study, the Matlab programs were designed based on the placement methodology explained in Section 5. The initial number of piezoelectric sensors equal to or less than 5% of the structure surface would be selected and placed at the most influential positions using genetic algorithms according to the placement methodology. The Matlab program was then utilised to optimise the location of piezoelectric transducers on a homogenous composite plate and plate stiffened by beam, as shown in Fig. 2. The stiffener is placed along one edge of the plate to make it dynamically asymmetrical. Damage was

inflicted by creating artificial cracks in several plates at different positions and orientations, which were tested in the "healthy" and "unhealthy" states with sensors located according to the chromosomes of the test population as directed by the genetic algorithm program. The healthy and unhealthy plates were modelled and represented using Ansys Parametric Desing Language (APDL) programming to get the piezoelectric sensors' voltage-frequency responses. The effectiveness of sensors in damage detection was evaluated using conventional $NRMSD$ and proposed $RMSD$ damage indices, while the optimal number and positions of sensors were determined based on the proposed normal damage index $RMSD^{nor}$. Another proposed normal damage index $NRMSD^{nor}$ would be used for further investigation and comparison.

6.1 Research problem description

The first stage of genetic algorithms placement methodology is utilised for cantilever composite flat plate and stiffened plate by beam dimensions 380×290×2 mm, as shown in Figure 2. Table 1 shows the properties of the plate and the piezoelectric sensors. The flat plate's modal dynamic strain is symmetric about a single axis and asymmetric for the stiffened plate. MFC sensors of dimensions of 20×20×0.3 mm were selected to be bonded to the plates' surface. An initial number of six piezoelectric sensors representing 4.5% of plate surface area were chosen to be located optimally based on the placement methodology.

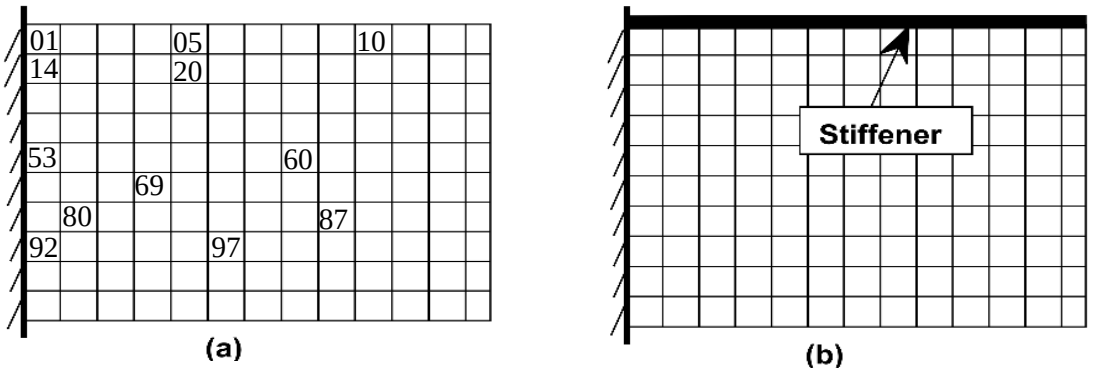

Fig.2. Rectangular plates with mounted as cantilevers on the left hand edge showing the distribution of potential sensor sites:
(a) a simple flat plate
(b) the same plate stiffened by a beam along one edge.

The plates' surface was discretised into one hundred thirty sub-areas representing 13×10 locations, sequentially numbered from left to right and up to down, as shown in Figure 2. The chromosomes are coded by a string of integer numbers based on the number of sensors required to be optimised and positions on the plate surface. Examples of chromosomes coded by a string of integer numbers to locate six sensors for both plates shown in Figure (2) are [01 60 80 10 97 53]. The total number of generated chromosomes for an optimisation problem is determined based on the statistical combinations of two

numbers: the total number of positions on the plate's surface and the number of sensors required to be optimised.

Table 1 Composite plate, stiffener, MFC sensor properties.

Properties	Plate and stiffeners	MFC type d31
E_x, E_y, E_z (GPa)	51.76, 46.54, 9.68	---------
G_{xy}, G_{yz}, G_{xz} (GPa)	4.945,4.945,14.27	---------
$\mu_{xy}, \mu_{yz}, \mu_{xz}$	0.475, 0155, 0.153	---------
Density (Kg/m^3)	1540	5440
e_{31}, e_{32}, e_{33} (C/m^2)	---------	-7.12, -4.53,12.1
$C_{11}^E, C_{12}^E, C_{13}^E, C_{55}^E$ (GPa)	---------	39.4,12.9,8.3,5.5
μ_{33}^{σ} (F/m)	---------	1.27×10^{-8}

6.2 Natural frequency

Both composite plates were modelled using the ANSYS finite element package to determine the first twelve natural frequencies. Table 2 shows the first twelve natural frequencies for the two composite plates with and without sensors in the optimal locations. Adding the mass and the stiffness of the MFC sensors to the main structure has the effect of reducing and increasing the natural frequencies, respectively.

Table 2 Natural frequencies for the plates with and without MFC piezoelectric sensors.

Natural frequencies of the flat plate (Hz)		Natural frequencies of the stiffened plate (Hz)	
Without MFCs	With MFCs	Without MFCs	With MFCs
13.867	14.097	18.383	19.354
24.925	25.200	81.742	83.769
83.970	85.170	93.363	97.588
102.93	104.21	173.27	176.53
147.90	148.10	174.42	179.01
213.63	214.84	235.83	249.20
245.76	248.70	319.07	332.03
253.33	256.40	360.43	362.98
362.16	365.11	384.19	383.67
394.47	394.95	458.07	480.80
459.43	460.52	524.24	536.39
475.32	480.56	545.21	570.83

The results of natural frequencies for both plates shown in Table 2 are all slightly increased, indicating that the stiffening effect dominates over the added mass effect. In addition, the table shows the significant impact of the stiffener beam on the natural frequencies of the plate.

6.3 Optimal placement of sensors for a cantilever plate

A Matlab m-file was designed based on the method set out in Section 5. The optimal locations for six piezoelectric sensors were determined for a rectangular plate, and a similar plate stiffened along one edge. Both were mounted as cantilevers along one edge and excited into vibration at each of their first twelve natural frequencies by the imposed out-of-plane motion on the mounting edge.

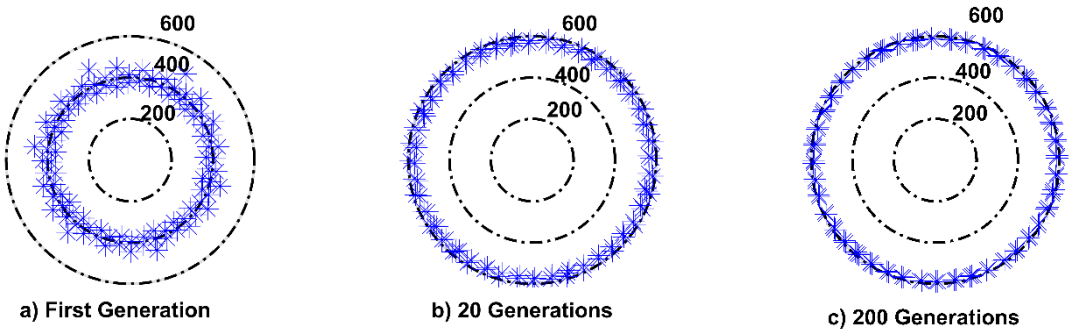

Fig.3. Population fitness progression over 200 generations. Each individual is represented as one of the points distributed around the circle, with its fitness values, obtained from its chromosome, defining its distance from the centre with large radius indication of high fitness

The progressive improvement of "fitness", as defined by equation 23, is shown in Figure 3, in which the radius of a point represents the fitness value for each chromosome. At the first generation, with random values for the genes on each chromosome and hence random sensor locations defined by them, there is a wide scatter of low fitness levels. After twenty generations, the scatter is reduced, and the overall fitness level is greatly improved. Finally, after two hundred generations, the population has converged to a high fitness level, indicating that the GA has found the best distribution of the six sensors for measuring the twelve resonant vibration modes.

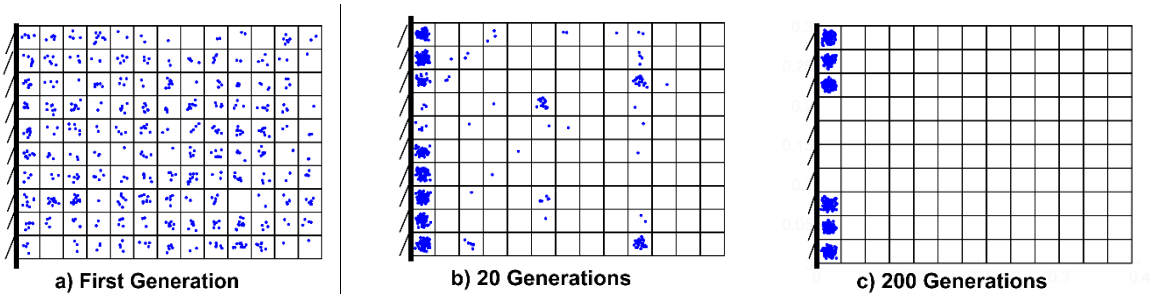

Fig. 4. Sensor placement for the cantilever composite plate. Each dot shows the location of a sensor in one of the 100 breeding individuals in each generation. Initially, they are randomly distributed. After twenty generations, they have begun to group in efficient locations. After 200 generations, they have fully converged on six optimal sites at the root of the plate.

Figure 4 presents the same results for the unstiffened plate in another form. The dots represent a sensor position as defined by the genes in all the chromosomes of a given generation. At the first generation with the initial random setting of the genes, the sensor locations are well distributed. After twenty generations the GA has started to concentrate the sensor locations away from ineffective sites, and after two hundred generations, it has converged onto six locations close to the mounting edge, which intuition also suggests would be positions of high strain for all modes for this simple case and confirms the results shown in Figure 4. Figure 5 shows the optimal locations for six sensors obtained by the genetic algorithms, first on the unstiffened plate and then for the plate made dynamically asymmetrical by means of the stiffener on one edge.

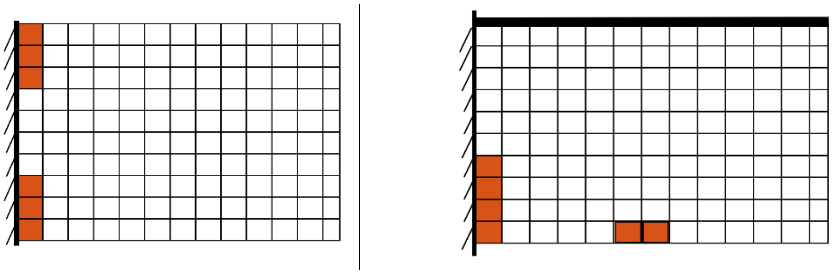

Fig. 5. The results of the current work for the optimal six sensors placement for the cantilever flat and stiffened plates

6.4 Results convergence

A possible flaw in any optimisation method is known as "premature convergence", where a local optimum is found rather than the overall global optimum. To test for this possibility, the GA was run six times over sixty generations, and the results are shown in Figure 6.

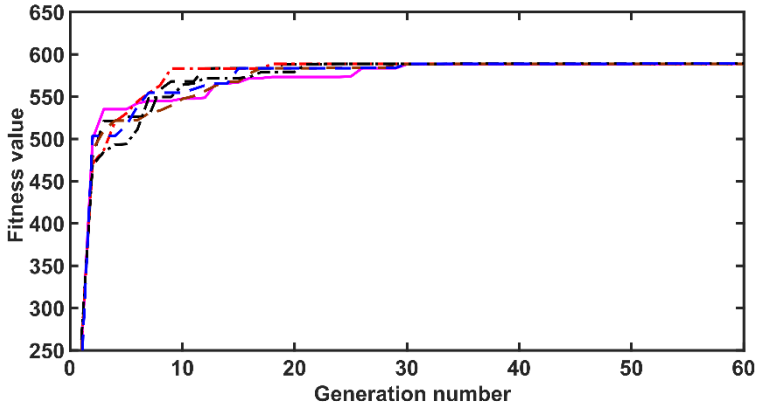

Fig. 6. Fitness value for the best individual in each generation repeated for six times for the cantilever plate to optimise six sensors. The figure shows different path at each run ending with same fitness value.

As expected, the runs behaved differently in the early generations but converged to the same fitness value, obtained from the same optimal sensor locations, in each case. This effectively validates the proposed placement methodology using the genetic algorithm for this application.

6.5 Optimal placement and number of transducers

6.5.1 Sensor voltage amplitude-frequency responses for healthy and damaged plates

According to the second stage of the placement methodology, a healthy plate and twelve damaged plates were bonded with MFC sensors to the surface of the plates at locations Sn1-Sn7 shown in Figure 7, where Sn1-Sn6 are the previously determined optimal sites, Sn7 was located arbitrarily for comparison. The piezoelectric transducers at location Sn5 was used as an actuator to excite all the plates with a sinusoidal voltage amplitude of 50 V at frequencies 10-500Hz. Twelve damaged plates were created, each with one 20×0.5mm artificial crack in the *x* or *y* direction (CKx1-CKx6 and CKy1-CKy6 in figure 7b). The Ansys Parametric Design Language (APDL) models for these plates used three-dimensional solid95 elements for the passive plate structure and solid226 for the active piezoelectric transducers. These were used to determine the voltage amplitude-frequency responses for the sensors in each case.

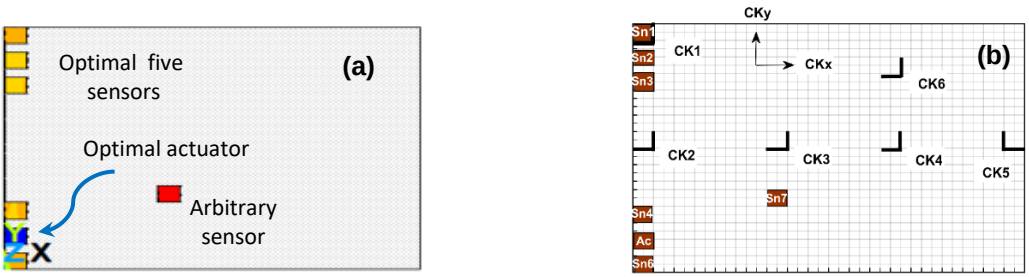

Fig. 7. (a) cantilever plate mounted rigidly from left side bonded with five piezoelectric sensors Sn1, Sn2, Sn3, Sn4 and Sn6 and one actuator located optimally, one sensor Sn7 located randomly and (b) distribution of twelve artificial cracks, made in x- and y-directions in twelve damaged plates, a single crack on each of them.

Figures 8 and 9 show the results of sensor voltage amplitude at the frequency domain of the healthy and cracked plate measured by one of the optimally placed sensors Sn2 with cracks in the x- and y-directions, respectively. These figures show that the cracked plates' peaks amplitude and frequencies deviate from the healthy plate's peaks. The degree of deviations are affected by the sensor location, crack position, crack direction and fundamental frequencies. The cracks in y-direction show a deviation in fundamental frequencies and amplitude, according to Figure 9. In contrast, the cracks in x-direction show a deviation in just amplitude, according to Figure 8.

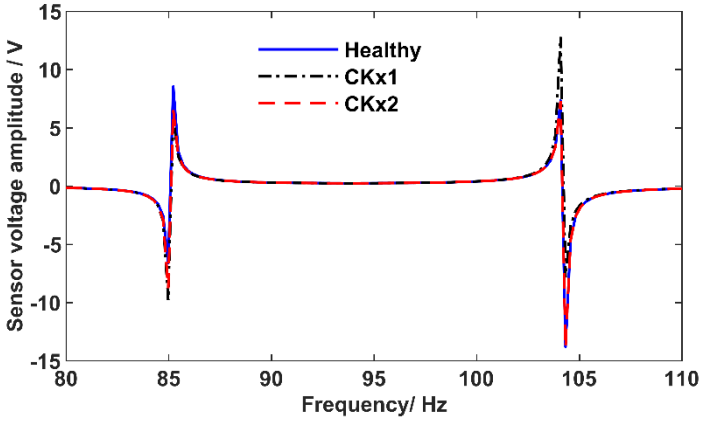

Fig. 8. Sensors voltage frequency responses at location 02 for the healthy and unhealthy plates with different cracks location in the x-direction.

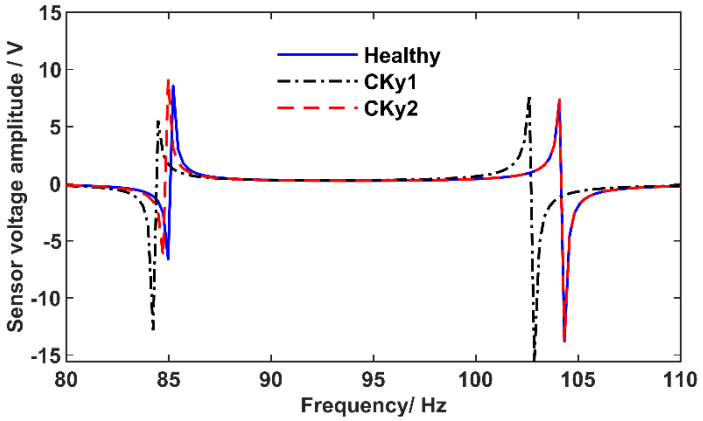

Fig. 9. Sensors voltage frequency responses at location 02 for the healthy and unhealthy plates with different cracks location in the y-direction.

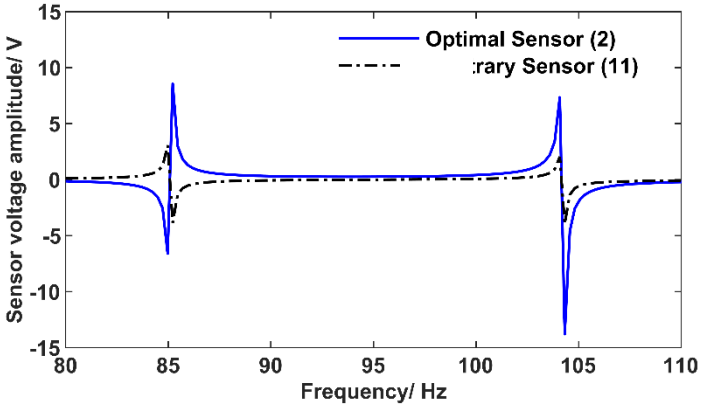

Fig. 10. Sensor voltage frequency responses for the sensor located optimally at the position Sn2 and arbitrary location Sn7.

Figure 10 shows frequency responses for the healthy plate as measured by the optimally placed sensor Sn2, and the arbitrarily placed sensor Sn7. It can be seen that a higher voltage amplitude-frequency response for the optimal sensor location than the arbitrary sensor location since the optimal

sensor locations were selected based on the maximisation of the output sensor voltage as an objective function at the first stage of the placement method. Physically, the modal strain intensity at the position of the optimum sensor location is higher than the arbitrary location, leading to higher voltage generation. The results show that the voltage response of a single optimally located piezoelectric sensor is sensitive to crack position and orientation, which indicates a promising damaging evaluation framework for SHM.

6.5.2 Damage evaluation

A quantitative damage evaluation was studied based on the sensors voltage amplitude-frequency responses measured at the various sensor locations described in Section 5.5.1, using the proposed RMSD and the conventional NRMSD indices explained in Section 3. These results are shown in Tables (3) and (4), respectively.

In Table (3), the RMSD damage evaluation index results may be seen to be affected by the position and direction of the cracks and the location of the sensors. Generally, the RMSD values for the y-direction cracks (perpendicular to the axis of symmetry) are larger than for the x-direction cracks in the same position, with the exception of the crack at position 5 close to the free end of the plate. Also, the RMSD values obtained from the optimum sensors are more significant than from the arbitrarily placed sensor Sn7. The RMSD values for the optimal sensors located above the symmetry axis are quite similar to those located below for both cracks in the x and y-direction. The RMSD for sensors Sn1 and Sn6 are 77.9%/78.0% respectively for crack CKx1, and 117.2%/117.5% for CKy1, even though the actuator location was located close to Sn6 and the cracks close to Sn1. This indicates the symmetry of the dynamic strain intensity at both sensors Sn1 and Sn6, and the damage index is not affected by cracks or actuating position. It can be concluded and reported that the symmetry of the RMSD damage evaluation index for the symmetrical structure in geometry and boundary condition is not affected by the distance between the cracks, optimal sensor and actuator locations for a structure bonded with optimally located sensor and actuator.

The percentage of the RMSD is reduced gradually from the root to the free-end plate because of the reduction in the dynamic strain intensity. It may be seen that the RMSD damage evaluations are mostly affected by the sensor location, strain intensity and crack direction. It can be noticed that a sensor close or next to a crack does not necessarily make it more effective in detecting the crack. For example, it can be observed from Table 3 that the damage index RMSD obtained from all the optimally located sensors Sn1, Sn2, Sn3, Sn4 and Sn6 are larger than that for the arbitrarily located sensor, even though Sn7 is the closest sensor to the crack at position 3.

Table 3 Results of the percentage (RMSD) for the twelve damaged plates.

Damaged Plates	Percentage of the proposed (RMSD) damage index					
	Optimal sensor location according to Fig. (7)					Random
	Sn1	Sn2	Sn3	Sn4	Sn6	Sn7
Plate1/CKx1	77.9	67.2	49.6	49.9	78.0	17.4
Plate2/CKx2	22.0	18.6	15.2	15.5	22.4	7.91
Plate3/CKx3	36.6	21.2	11.1	11.2	36.8	18.1
Plate4/CKx4	35.4	19.9	9.9	10.0	35.6	17.5
Plate5/CKx5	125	110	84.5	85.3	125	44.8
Plate6/Ckx6	15.9	15.7	16.6	15.9	15.7	19.6
Plate7/CKy1	117.2	136.6	99.3	106	117.5	47.5
Plate8/CKy2	79.7	75.1	64.3	65.5	81.3	35.8
Plate9/CKy3	58.0	52.5	45.1	46.2	59.3	32.1
Plate10/CKy4	57.2	50.6	43.2	44.3	58.4	30.8
Plate11/CKy5	9.71	8.31	6.6	6.8	9.8	3.43
Plate12/CKy6	106.3	98.6	76.6	78.3	108.5	39.6

Also, the damage index recorded by Sn1 is larger than Sn2 and Sn3 for crack damage at position 2, though Sn2 and Sn3 are closer to the crack at position 2. Finally, Table 3 shows all the optimally placed sensors performed much better at damage detection than the arbitrarily located sensor Sn7 for all the cracks in both directions, though Sn7 is the closest to four of the six crack sites, i.e crack positions 3, 4, 5 and 6. This finding is in agreement with that of Soni et al investigating SHM of a lug joint in an aerospace structure at ultrasonic frequencies with a piezoelectric actuator and five sensors arbitrary located around 20 mm and 40mm crack, who observed that some sensors located far away from a crack performed better than some closer sensors in both simulation and experimental test (Soni, Das and Chattopadhyay, 2009).

Table 4 Results of the percentage NRMSD for the twelve damaged plates.

Damaged Plates	Percentage (NRMSD) damage index					
	Optimal sensor location, see Fig. (7)					Random
	Sn1	Sn2	Sn3	Sn4	Sn6	Sn7
Plate1/CKx1	73.5	70	66.8	65.2	71.6	46.5
Plate2/CKx2	20.7	19.4	20.4	20.3	20.5	21.1
Plate3/CKx3	34.6	22.1	14.9	14.7	33.8	48.5
Plate4/CKx4	33.4	20.7	13.3	13.0	32.7	46.9
Plate5/CKx5	118	114.5	113.7	111.3	115.5	119.7
Plate6/Ckx6	15	16.4	22.4	20.7	14.4	52.5
Plate7/CKy1	110.6	142.3	133.6	138.3	139.4	127
Plate8/CKy2	75.2	78.2	86.5	85.5	74.6	95.8
Plate9/CKy3	54.8	54.7	60.7	60.2	54.5	85.8
Plate10/CKy4	54.0	52.7	58.2	57.8	53.6	82.5
Plate11/CKy5	9.1	8.6	9.00	8.9	9.0	9.1
Plate12/CKy6	100	102	103	102.2	99.6	105

However, these findings obtained using the proposed non-normalised damage evaluation index $RMSD$ are not apparent in the results obtained using the normalised index $NRMSD$ shown in Table 4. For instance, the $NRMSD$ values for crack positions CKx2, CKx5, CKy5 and CKy6 are the same for all sensors, and the $NRMSD$ value for the arbitrary sensor Sn7 is larger than for optimal sensors for all the cracks because the value the denominator of the $NRMSD$ formula is equal to the sensor voltage multiply by itself. This makes the result of the $NRMSD$ very high when the response voltage amplitude is low at the randomly located sensor Sn7, as shown in Figure 10. The $NRMSD$ damage index results for arbitrary sensor location is conflicted with the piezoelectric sensor optimisation scheme and misled damage evaluation. Furthermore, the normalised damage index $NRMSD$ cannot differentiate between the effectiveness of the sensor position for damage detection, whereas the non-normalised $RMSD$ can differentiate very effectively.

6.5.3 Optimal number of piezoelectric transducer

The most effective piezoelectric transducers in damage detection were selected based on the proposed average normal damage index $RMSD^{nor}$ as the objective function explained in Sections 5.2. Another normal damage index $NRMSD^{nor}$ was proposed for deep investigation and comparison. Tables 5 and 6 shows the results of both normal damage indices measured for twelve plates cracked at different positions and orientations based on the results obtained in Section 5.5.3. Table 5 shows that the maximum average normal damage index $RMSD^{nor}$ for the twelve plates at the optimal sensor locations are 96.1 and 97.1 at Sn1 and Sn6, respectively. Thus, the maximum values of the normal damage index for Sn1 and Sn6 demonstarte the effectiveness of the proposed placement methodology and these transducers in detecting cracks covering the whole plate's surface area. Therefore, these two sensors Sn1 and Sn6 are selected as the optimal number and placement to achieve the optimality and simplicity of the active SHM system. The optimal number and placement of these two sensors Sn1 and Sn6 were selected based on the proposed objective function in eq. (27). On the other hand, the results in Table 5 shows that the minimum average value $RMSD^{nor}$ at the arbitrary sensor location, Sn7 is 45.7, as usually expected for the sensor located randomly. The scientific interest of the results is represented by the testing of the effectiveness of the fitness, objective functions and placement methodology in determining the optimum number and placement of piezoelectric sensors at the low computational effort. Determination of the optimum number and positions of piezoelectric transducers in the earliest design stage of the SHM system promises a positive impact on the cost, data acquisition and processing, and effectiveness of the SHM system.

Table 6 shows the average normal damage index $NRMSD^{nor}$ for the twelve damaged plates. It can be noticed from Table 6 that the maximum average normal damage index $NRMSD^{nor}$ is 96.0 for the sensor Sn7 located randomly, while the results for all optimal sensors are accumulated between

75.4-79.7. These results are breached the concept of optimisation as the maximum value is assigned to the random sensor position Sn7 as the causes are explained in the last paragraph in Section 5.5.2 and 5.3. The results for both conventional $NRMSD$ and proposed $NRMSD^{nor}$ are misled the cracks detect, evaluation and piezoelectric sensor placement, while the proposed damage index $RMSD$ and $RMSD^{nor}$ are most effective to differentiate the results of the sensors' responses.

Table 5 Results of the Normal ($RMSD^{nor}$) for the twelve damaged plates.

Damaged Plates	Proposed Normal ($RMSD^{nor}$) damage index					
	Optimal sensor location, see Fig. (7)					Random
	Sn1	Sn2	Sn3	Sn4	Sn6	Sn7
Plate1/CKx1	99.8	86.1	63.6	63.9	100	22.3
Plate2/CKx2	98.2	83.0	15.2	67.8	100	35.3
Plate3/CKx3	99.4	57.6	30.1	30.43	100	49.1
Plate4/CKx4	99.4	55.8	27.8	28.0	100	49.1
Plate5/CKx5	100	88.0	67.6	68.2	100	35.8
Plate6/Ckx6	81.1	80.1	84.6	81.1	80.1	100
Plate7/CKy1	85.7	100	72.6	77.5	86.0	34.7
Plate8/CKy2	98.0	92.3	79.0	80.5	100	44.0
Plate9/CKy3	97.8	88.5	76.0	77.9	100	54.3
Plate10/CKy4	97.9	86.6	73.9	75.8	100	52.7
Plate11/CKy5	99.0	84.8	67.3	69.3	100	35.0
Plate12/CKy6	97.9	90.8	70.5	72.1	100	36.4
Average $RMSD^{nor}$	**96.1**	82.8	60.6	66.0	**97.1**	45.7

The piezoelectric sensors Sn1 and Sn6 are selected to be the optimal number and placement for the cantilever plate according to equation 27, their $J^N(x,y)$ values are 96.1 and 97.1

Table 6 Results of the Normal ($NRMSD^{nor}$) for the twelve damaged plates.

Damaged Plates	Normal damage index ($NRMSD^{nor}$)					
	Optimal sensor location, see Fig. (7)					Random
	Sn1	Sn2	Sn3	Sn4	Sn6	Sn7
Plate1/CKx1	100	95.2	90.9	88.7	97.4	63.3
Plate2/CKx2	98.1	91.9	96.7	96.2	97.2	100
Plate3/CKx3	71.3	45.6	30.7	30.3	69.7	100
Plate4/CKx4	71.2	44.1	28.4	27.7	69.7	100
Plate5/CKx5	98.6	95.7	95.0	93.0	96.5	100
Plate6/Ckx6	28.6	31.2	42.7	39.4	27.4	100
Plate7/CKy1	77.7	100	93.9	97.2	98.0	89.3
Plate8/CKy2	78.5	81.6	90.3	89.3	77.9	100
Plate9/CKy3	63.9	63.8	70.8	70.2	63.5	100
Plate10/CKy4	65.5	63.9	70.6	70.1	65.0	100
Plate11/CKy5	100.0	94.5	98.9	97.8	98.9	100
Plate12/CKy6	95.2	97.1	98.1	97.3	94.9	100
Average $NRMSD^{nor}$	79.0	75.4	75.6	74.8	79.7	**96.0**

The $J^N(x,y)$ for the arbitrary sensor Sn7 displayed the maximum value of 96.0, which conflicts with the optimal sensor placement scheme and misleads damage detection and evaluation.

CONCLUSION

In this study, new fitness and objective functions and a two-stage placement methodology have been proposed to reduce the complexity and optimise the cost of data acquisition for active SHM systems, which was achieved by determining optimal number and location of piezoelectric transducers using genetic algorithms. Maximisation of sensor voltage and the normal damage index ($RMSD^{nor}$) were proposed as objective functions to find the placement and number of piezoelectric sensors. The root mean square deviation $RMSD$ damage index was introduced in this study to eliminate the drawback effects of the conventional normalised $NRMSD$ damage index. In addition new normal damage indices, i.e, $RMSD^{nor}$ and N$RMSD^{nor}$ normalised to 100% are proposed.

The placement methodology is utilised to unstiffened and stiffened composite plates bonded with the initial six MFC sensors covering 4.5% of the plate surface. The resulting optimal distribution of the six transducers at the first stage of the optimisation process were verified by running the genetic algorithms multiple times were ended to the identical optimal chromosome, though the convergence progression took different paths. The optimal number and placement of piezoelectric sensors were investigated using the second stage placement methodology. The second stage was tested on a healthy plate and twelve damaged plates with artificial cracks made at various positions and orientations using Ansys finite element package.

This study provides a useful tool for both researchers and engineers to optimise active SHM systems for optimal number and placement of piezoelectric transducers. It will also help industrial companies to optimise the cost, data acquisition and effectiveness of the SHM system at the earliest design stage. It is worthy of noting, this study is limited to structures bonded with piezoelectric transducers and subjected to low frequencies. Therefore, it needs to be tested and modified for the same structures bonded with piezoelectric transducers and subjected to ultrasonic frequencies and structures bonded with accelerometer sensors under low frequencies. The findings of this study are summarised as followings:

1. The proposed fitness functions, objective functions and the two-stage placement methodology are efficient in determining the optimum number and positions of piezoelectric sensors at a low computational effort, enabling the cost, data acquisition and processing at a minimum level for active SHM systems.
2. The optimally placed piezoelectric transducers have higher $RMSD$ and $RMSD^{nor}$ damage evaluation indices than the arbitrarily placed sensors for all the cracks tested in different orientations at different positions.

3. It is shown that a piezoelectric sensor located optimally performs more effectively for damage detection and evaluation than one located close to the defect. Sensors located close to cracks did not necessarily make them more effective in detecting cracks.
4. For symmetric structures in geometry and boundary conditions, cracks have only a small effect on the dynamic symmetry. Therefore, the responses of symmetric sensors located optimally are virtually symmetric in voltage and damage evaluation index, especially at the initiation stage of cracking.
5. It is shown that the proposed $RMSD$ and $RMSD^{nor}$ indices performed better as indicators of damage than conventional $NRMSD$ and $NRMSD^{nor}$.
6. The $NRMSD$ and $NRMSD^{nor}$ damage indices are conflicted with the sensor optimisation scheme and misled crack evaluation and the optimal piezoelectric sensor positions.

REFERENCES

Ai, D., Zhu, H. and Luo, H. (2016) 'Sensitivity of embedded active PZT sensor for concrete structural impact damage detection', *Construction and Building Materials*. Elsevier Ltd, 111, pp. 348–357.

Balamonica, K., Jothi Saravanan, T., Bharathi Priya, C. and Gopalakrishnan, N. (2020) 'Piezoelectric sensor–based damage progression in concrete through serial/parallel multi-sensing technique', *Structural Health Monitoring*, 19(2), pp. 339–356.

Buff, H., Friedmann, A., Koch, M., Bartel, T. and Kauba, M. (2012) 'Design of a random decrement method based structural health monitoring system', 19, pp. 787–794.

Chalioris, C.E., Papadopoulos, N.A., Angeli, G.M., Liolios, A.A. and Providakis, C.P. (2015) 'Damage Evaluation in Shear-Critical Reinforced Concrete Beam using Piezoelectric Transducers as Smart Aggregates', *Open Engineering*, 5(1), pp. 373–384.

Daraji, A. H. and Hale, J. M. (2012) 'Active vibration reduction of a flexible structure bonded with optimised piezoelectric pairs using half and quarter chromosomes in genetic algorithms', *Journal of Physics: Conference Series*, 382, p. 012039.

Daraji, A. H. and Hale, J. M. (2014) 'Active vibration reduction by optimally placed sensors and actuators with application to stiffened plates by beams', *Smart Materials and Structures*, 23(11),115018.

Daraji, A. H., Hale, J. M. and Ye, J. (2018) 'New Methodology for Optimal Placement of Piezoelectric Sensor/Actuator Pairs for Active Vibration Control of Flexible Structures', *Journal of Vibration and Acoustics, Transactions of the ASME*, 140(1), p.011015.

Doebling, S. W., Farrar, C. R., Prime, M. B., and Shevitz, D. W. (1996) 'Damage identification and health monitoring of structural and mechanical systems from changes in their vibration characteristics: A literature review', Los Alamos National Labrotory, New Mexico.

Fan, S., Zhao, S., Qi, B. and Kong, Q. (2018) 'Damage evaluation of concrete column under impact load using a piezoelectric-based EMI technique', *Sensors (Switzerland)*, 18(5), p.1591.

Flynn, E. B. and Todd, M. D. (2010a) 'A Bayesian approach to optimal sensor placement for structural health monitoring with application to active sensing', *Mechanical Systems and Signal Processing*. Elsevier, 24(4), pp. 891–903.

Flynn, E. B. and Todd, M. D. (2010b) 'Optimal placement of piezoelectric actuators and sensors for detecting damage in plate structures', *Journal of Intelligent Material Systems and Structures*, 21(3), pp. 265–274.

Gillich, G.-R., Furdui, H., Abdel Wahab, M. and Korka, Z. I. (2019) 'A robust damage detection method based on multi-modal analysis in variable temperature conditions', *Mechanical Systems and Signal Processing*. Elsevier Ltd, 115, pp. 361–379.

Goldberg D. E. (1989) ' *Genetic Algorithms in Search, Optimisation and Machine Learning*', Addison-Wesley, USA

Guo, F., Yu, Z., Liu, P. and Shan, Z. (2016) 'Practical Issues Related to the Application of Electromechanical Impedance-Based Method in Concrete Structural Health Monitoring', *Research in Nondestructive Evaluation*, 27(1), pp. 26-33.

Han, J.-H. and Lee, I. (1999) 'Optimal placement of piezoelectric sensors and actuators for vibration control of a composite plate using genetic algorithms', *Smart Materials and Structures*, 8(2), pp. 257–267.

He, C., Xing, J., Li, J., Yang, Q., Wang, R. and Zhang, X. (2013) 'A combined optimal sensor placement strategy for the structural health monitoring of bridge structures', *International Journal of Distributed Sensor Networks*, p. 820694.

Khatir, S., Abdel Wahab, M., Boutchicha, D. and Khatir, T. (2019) 'Structural health monitoring using modal strain energy damage indicator coupled with teaching-learning-based optimization algorithm and isogoemetric analysis', *Journal of Sound and Vibration*, 448, pp. 230–246.

Khatir, S., Boutchicha, D., Le Thanh, C., Tran-Ngoc, H., Nguyen, T.N. and Abdel-Wahab, M. (2020) 'Improved ANN technique combined with Jaya algorithm for crack identification in plates using XIGA and experimental analysis', *Theoretical and Applied Fracture Mechanics*. Elsevier, 107(February), p. 102554.

Khatir, S. and Abdel Wahab, M. (2019) 'Fast simulations for solving fracture mechanics inverse problems using POD-RBF XIGA and Jaya algorithm', *Engineering Fracture Mechanics*. Elsevier, 205(September 2018), pp. 285–300.

Kong, Q., Robert, R.H., Silva, P. and Mo, Y.L. (2016) 'Cyclic Crack Monitoring of a Reinforced Concrete Column under Simulated Pseudo-Dynamic Loading Using Piezoceramic-Based Smart Aggregates', *Applied Sciences*, 6(11), p. 341.

Lee, C. and Park, S. (2012) 'De-Bonding Detection on a CFRP Laminated Concrete Beam using Self Sensing-Based Multi-Scale Actuated Sensing with Statistical Pattern Recognition', *Advances in Structural Engineering,*

15(6), pp. 919-927.

Li, D. S., Li, H. N. and Fritzen, C. P. (2012) 'Load dependent sensor placement method: Theory and experimental validation', *Mechanical Systems and Signal Processing*. Elsevier, 31, pp. 217–227.

Lu, W., Wen, R., Teng, J., Li, X. and Li, C. (2016) 'Data correlation analysis for optimal sensor placement using a bond energy algorithm', *Measurement: Journal of the International Measurement Confederation*. Elsevier Ltd, 91, pp. 509–518.

Markmiller, J. F. C. and Chang, F. K. (2010) 'Sensor network optimization for a passive sensing impact detection technique', *Structural Health Monitoring*, 9(1), pp. 25–39.

Mehrjoo, M., Khaji, N. and Ghafory-Ashtiany, M. (2013) 'Application of genetic algorithm in crack detection of beam-like structures using a new cracked Euler-Bernoulli beam element', *Applied Soft Computing Journal*. Elsevier B.V., 13(2), pp. 867–880.

Ostachowicz, W. and Soman, R. (2019) 'Optimization of sensor placement for structural health monitoring : a review'. Structural Health Monitoring, 18(3), pp. 963-988.

Park, S., Ahmad, S., Yun, C.-B. and Roh, Y. (2006) 'Multiple Crack Detection of Concrete Structures Using Impedance-based Structural Health Monitoring Techniques', Experimental Mechanics, 46(5), pp. 609–618.

Perera, R., Gil, A., Torres, L. and Barris, C. (2021) 'Diagnosis of NSM FRP reinforcement in concrete by using mixed-effects models and EMI approaches', *Composite Structures*, 273, p. 114322.

Kumar, K. R. and Narayanan, S. (2007) 'The optimal location of piezoelectric actuators and sensors for vibration control of plates', *Smart Materials and Structures*, 16(6), pp. 2680-2691.

Kumar, K. R. and Narayanan, S. (2008) 'Active vibration control of beams with optimal placement of piezoelectric sensor/actuator pairs', *Smart Materials and Structures*, 17(5), p. 055008.

Sadri, A. M., Wright, J. R. and Wynne, R. J. (1999) 'Modelling and optimal placement of piezoelectric actuators in isotropic plates using genetic algorithms', *Smart Materials and Structures*, 8(4), pp. 490–498.

Song, G., Gu, H., Mo, Y.L., Hsu, T.T.C. and Dhonde, H. (2007) 'Concrete structural health monitoring using embedded piezoceramic transducers', *Smart Materials and Structures*, 16(4), pp. 959–968.

Song, H., Lim, H. J. and Sohn, H. (2013) 'Electromechanical impedance measurement from large structures using a dual piezoelectric transducer', *Journal of Sound and Vibration*. Elsevier, 332(25), pp. 6580–6595.

Soni, S., Das, S. and Chattopadhyay, A. (2009) 'Simulation of damage-features in a lug joint using guided waves', *Journal of Intelligent Material Systems and Structures*, 20(12), pp. 1451–1464.

Yang, H.-F., Wu, Z.-Y., Liu, S.-K. and Sun, H. B. (2012) 'Research on optimal sensor placement based on reverberation matrix for structural health monitoring', *International Journal of Distributed Sensor Networks*, p.454530.

Yang, Y. (2010) 'Sub-Frequency Interval Approach in Electromechanical Impedance Technique for Concrete Structure Health Monitoring', pp. 11644–11661.

Yi, T. H., Li, H. N. and Gu, M. (2011) 'Optimal sensor placement for health monitoring of high-rise structure based on genetic algorithm', *Mathematical Problems in Engineering*, p.395101.

Zhang, H., *Lennox, B., Goulding, P. R., and Leung, A. Y. T.* (2000) 'A float-encoded genetic algorithm technique for integrated optimization of piezoelectric actuator and sensor placement and feedback gains', *Smart Materials and Structures*, 9(4), pp. 552–557.

Zhou, G.-D., Yi, T.-H., Zhang, H. and Li, H.-N. (2015) 'A Comparative Study of Genetic and Firefly Algorithms for Sensor Placement in Structural Health Monitoring', *Shock and Vibration*, 2015, pp. 1–10.

Zhu, K., Gu, C., Qiu, J., Liu, W. and Fang, C., Li, B. (2016) 'Determining the Optimal Placement of Sensors on a Concrete Arch Dam Using a Quantum Genetic Algorithm', *Journal of Sensors*, p. 2567305.